Materials Advances

ROYAL SOCIETY OF CHEMISTRY

PAPER

View Article Online
View Journal | View Issue

Cite this: *Mater. Adv.*, 2026, 7, 4171

Auxetic polypropylene foams as high mechanical performance materials

Xiao Yuan Chen and Denis Rodrigue *

Received 14th November 2025,
Accepted 23rd January 2026

DOI: 10.1039/d5ma01329a

rsc.li/materials-advances

This study focuses on converting polypropylene (PP) foams into auxetic metamaterials using vacuum and mechanical compression (VMC). The PP foams (initial density of 45 kg m^{-3}) underwent treatments involving heat, vacuum and mechanical pressure to create a re-entrant cellular structure essential to generate a negative Poisson's ratio (NPR). The resulting foams exhibit significantly enhanced stiffness, making them suitable for applications in sports and military protection. The effect of vacuum and mechanical compression are optimized to achieve the best auxetic properties. The treated foams are characterized for density, porosity, open cell content (OCC), cell morphology, Poisson's ratio (ν) and mechanical properties. The optimized auxetic foams have high density (100–133 kg m^{-3}) and show NPR under both tensile (−0.23) and compressive (−0.08) deformation. More importantly, the toughness is improved by up to 438% compared to the original foam with a 200% increase of the elastic limit. Furthermore, the compression stress is improved by 416% at 50% compressive strain. Finally, thermo-mechanical data show that auxetic PP foams have improved properties as temperature increases.

1. Introduction

Metamaterials represent a fascinating class of materials known for their unconventional properties, derived from engineered microstructures. These materials exhibit non-conventional behaviors due to their unique geometric configurations and spatial distributions. One intriguing subset of metamaterials is auxetics, which are characterized by negative Poisson's ratios (NPR). These materials expand laterally when stretched and contract when compressed, which is the opposite behavior of most materials having positive PR.[1]

Auxetic foams have superior mechanical properties for a wide range of applications such as impact resistance, energy absorption, and high flexibility. These advantages also include:

1. Negative Poisson's ratio (NPR): auxetic foams exhibit improved stability and resistance to deformation under pressure, making them more robust in high-stress environments.

2. Enhanced energy absorption: this property is valuable in applications requiring impact protection, such as protective gear, packaging materials and automotive components, as auxetic foams can absorb and dissipate impact energy more effectively.

3. Improved toughness and resistance to fracture: the structure of auxetic foams improves durability, decreasing possibility of failure under high stress since they can better resist the propagation of cracks.

4. Increased shear modulus and damping: auxetic materials show higher shear modulus and damping factors, making them interesting for sound insulation, cushioning, and vibration control.

From these properties, auxetic foams are ideal for various applications in the medical field (prosthetics and orthotics), aerospace, construction and sports equipment where flexibility, durability and impact resistance are paramount.[2–4]

One method to produce auxetic polymer foams is to modify the standard cellular morphology to generate a re-entrant structure using different treatments. A re-entrant structure has cell walls with inward angle, a basic property for NPR. The methods available are based on thermal, physical, chemical and mechanical processes, which can be applied alone or combined together.[5] The transformation of conventional polymer foams into auxetic ones involves subjecting the foam to conditions such as heat treatment near the softening temperature of the matrix, followed by mechanical compression to deform the cellular structure, and finally cooling under compression to fix the re-entrant structure, thereby imparting auxetic properties.[5]

Researchers have successfully converted several types of polymer foams into auxetic materials, including polyamide (PA),[6] polypropylene (PP),[7] polystyrene (PS),[8] polyester (PES),[9] polyether urethane (PU),[10–16] polyvinyl chloride (PVC),[17] and various grades of polyethylene (PE).[18–21] These transformations lead to materials with enhanced elasticity and resistance to various types of deformation and stress.

Previous investigations reported that applying a vacuum and mechanical compression (VMC) are easy to perform to convert

Department of Chemical Engineering, Université Laval, Quebec, G1V0A6, Canada. E-mail: Denis.Rodrigue@gch.ulaval.ca

recycled polymer foams with NPR.[7,8,21] For example, low density (28 kg m^{-3}) recycled polypropylene (PP) foams were successfully converted into auxetic materials.[7] Here, the VMC method is used to convert conventional PP foams (45 kg m^{-3}) into auxetic metamaterials with enhanced toughness. Distinct from earlier reports on low density polyethylene (LDPE)[21] and polystyrene (PS)[8] foams, this work addresses the processing challenges associated with high density PP foams, exhibiting limited compressibility and higher resistance to permanent structural reconfiguration. This work not only focuses on the auxetic performance but also investigates the mechanical properties. The findings confirm the possibility of extending the VMC method to more rigid and less deformable polymer systems, thereby expanding its applicability for engineering auxetic metamaterials from higher density polymer foams. This improvement helps to increase their range of applications, including military, sports and leisure protective equipment. So this investigation explores the effect of mechanical stress, vacuum duration and compression level to optimize the final foam structure. The mechanical properties under tension and compression are measured to determine the PR, which is highly important for auxetic materials.

2. Materials and methods

2.1. Materials

Polypropylene (PP) foams was selected for this study. The starting material (planks) was bought from McMaster-Carr (USA).[22] The foam is composed of expanded polypropylene pellets compressed into a rigid board. This material is known for its high resistance to chemicals and moisture, a property attributed to the unique chemistry of PP. Nevertheless, the samples are composed of 90% PP and 10% carbon black (CB). The foams are initially produced by expanding polypropylene beads, leading to a cellular structure. The samples used had an initial density of 45 kg m^{-3} and dimensions of 120 cm × 60 cm × 25 mm. The treatments were performed using a vacuum oven (OVV-400-24-120 Programmable Vacuum Oven, 24 L, Cole-Parmer, Canada).

2.2. Methods

The PP foams underwent a series of treatments as follows. Initially, the material was cut into pieces of 10 cm × 10 cm × 2.5 cm using a doctor blade. Then, each sample was placed in a vacuum oven at 140 °C for 1 h. This temperature was selected to be close to the PP softening temperature (90–100 °C), but below its melting point (142 °C). Finally, vacuum (−0.88 bar) was imposed for different time (15–48 h) still at 140 °C, followed by a decompression step to return to ambient (1 atm) pressure. Mechanical pressure (0–9 kPa) was also applied by using metal blocks of different weights placed on the samples.

After treatment, each sample was left to cool inside the oven for 1–2 h under mechanical pressure.[7,8] The final volume of the foam produced during the VMC process was determined by a balance between the foam's expansion due to the elevated temperature and the vacuum/mechanical stress (weight) imposed. The initial density of the PP foam (PP-O) is 45 kg m^{-3}, which serves as the baseline for all the samples (Table 1). Each sample is coded with "PP" for the foam type, followed by "T" and a number indicating the treatment temperature (T140 for 140 °C), followed by a number representing the duration of vacuum treatment in hours (15–48 h), and finally "P" followed by the applied mechanical pressure in kilopascals (kPa). For instance, sample PP-T140-24-P5 refers to a PP foam treated at 140 °C for 24 h under a mechanical pressure of 5 kPa.

Table 1 Physical properties of the original and auxetic foams

Sample	Dimension (cm × cm × cm)	Density (kg m^{-3})	Porosity (%)	OCC (%)
PP-O	10 × 10 × 2.5	45 ± 1	95 ± 1	7.4 ± 0.1
PP-T140-24-P0	7.7 × 7.7 × 1.9	100 ± 4	89 ± 3	7.0 ± 0.3
PP-T140-24-P3	7.5 × 7.6 × 1.9	103 ± 6	89 ± 6	6.6 ± 0.4
PP-T140-24-P5	7.2 × 7.2 × 1.7	126 ± 3	86 ± 3	6.0 ± 0.4
PP-T140-24-P9	7.3 × 7.3 × 1.6	132 ± 8	86 ± 5	6.3 ± 0.4
PP-T140-18-P3	7.7 × 7.7 × 1.9	100 ± 5	90 ± 4	6.8 ± 0.3
PP-T140-48-P3	7.4 × 7.4 × 1.8	114 ± 10	87 ± 8	6.4 ± 0.5

2.3. Characterization

A detailed list of characterizations is reported in the SI, and more information can be obtained in a previous study.[21]

3. Results and discussion

3.1. Physical properties of the PP foams

Table 1 presents a summary of the physical properties of the foams, including dimensional changes, foam density, porosity and open cell content (OCC). According to Table 1, the dimensions of the samples decreased after processing. For example, the thickness decreased by 24–36%, while the length and width exhibited similar shrinkage (23–38%). Therefore, the contraction was relatively uniform in length, width and thickness.

The density of the auxetic foams increased initially with increasing mechanical pressure and treatment time. This behavior was expected because more pressure compresses more the foam, leading to higher final density (fixed time and temperature). But, longer time results in a higher-pressure differential across the cell walls to generate a more defined re-entrant structure with higher foam density. For example, PP-T140-48-P3 (114 kg m^{-3}) has a higher density compared to PP-T140-18-P3 (100 kg m^{-3}). Furthermore, the porosity of PP-T140-24-P0 (89%) is lower than that of PP-O (95%), but higher than that of PP-T140-24-P5 (86%) and other treated samples (86%). The open cell content (OCC) shows two distinct zones. The original PP foam had an OCC of 7.4%, whereas the treated samples had values ranging from 6% to 7%. This small variation indicates that the foam cells predominantly deformed into a re-entrant structure without cell rupture (no broken cell wall occurred).

3.2. Auxetic foams

3.2.1. Morphology. Fig. 1 presents typical SEM micrographs of the PP foam cross-sections, before and after

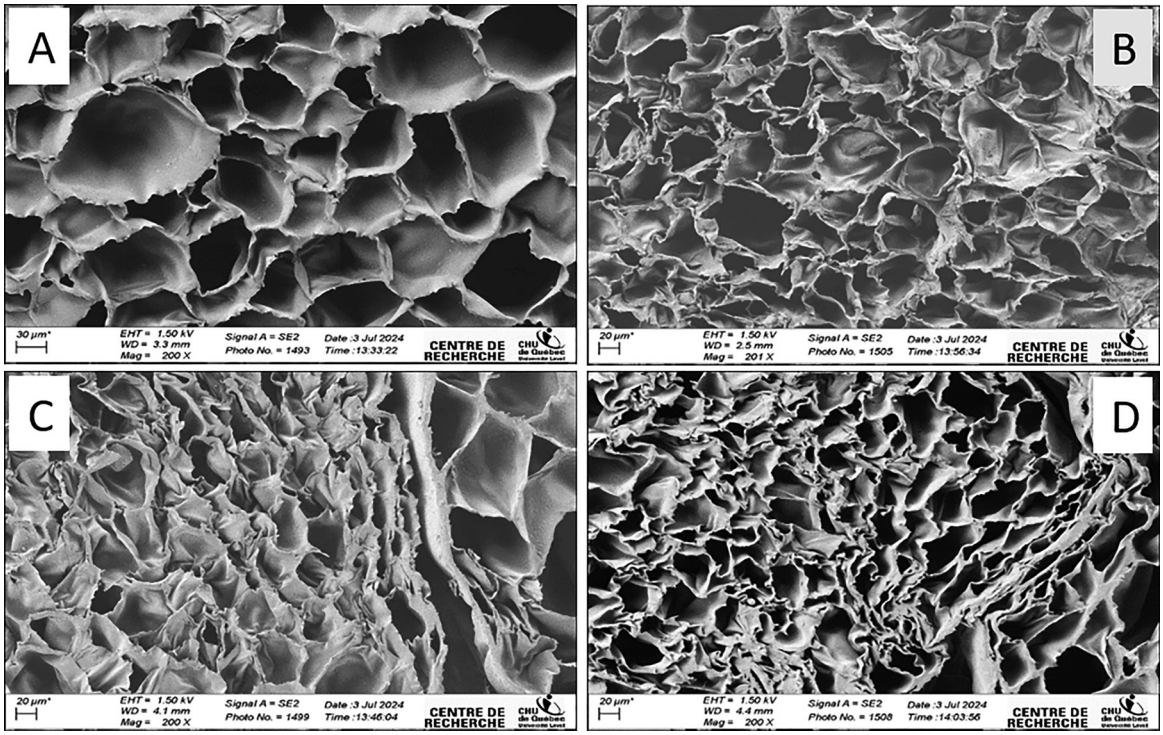

Fig. 1 Morphology (cross-section) of: (A) original foam (PP–O) as well as selected auxetic foams: (B) PP-T140-24-P0, (C) PP-T140-24-P3 and (D) PP-T140-24-P9.

modification. The original foam (Fig. 1A) displays a uniform distribution of small cells throughout the sample, mainly characterized by a closed-cell honeycomb structure. The average cell size was 165 ± 22 μm, similar as reported in the literature.[23,24]

From the treatments imposed, the cells show significant changes leading to a re-entrant structure. Fig. 1B has smaller cells compared to Fig. 1A, with some cells showing a re-entrant structure. Fig. 1C and D reveal that most cells collapsed inward, forming re-entrant structures making them challenging to measure the cell size due to their complex geometry. These samples were prepared under the same time and temperature, but using different mechanical pressure. Despite these differences, their structures remained similar.

3.2.2. Mechanical properties

3.2.2.1. Stress–strain curves. Fig. 2 compares the stress–strain curves in tension for both the original and auxetic foams (before and after treatment). These curves illustrate the relationship between engineering stress and engineering strain during tensile testing. The corresponding mechanical properties, including tensile modulus, tensile strength and strain at break, as well as toughness and elastic limit are summarized in Table 2.

As expected, both the Young's modulus and tensile strength increase with increasing density as more material is available to withstand the applied stresses. This relationship is directly proportional to the amount of material (density) present, as reported in the literature.[12,25,26]

On the other hand, the elongation at break decreases with increasing density. Nevertheless, the auxetic foams have higher elongation at break (13.9% to 28.7%) compared to the original foam (8.6%), indicating that they have higher ductility; *i.e.* greater ability to deform under tensile stress before failure.

Toughness refers to a material's ability to absorb energy before failure. For auxetic foams, increasing their density usually generates improved toughness. For instance, PP-T140-24-P5 has a toughness of 5.76 MPa, which is a 438% improvement compared to PP–O (1.07 MPa). This is due to the auxetic foam's unique internal structure, which distributes the stresses more evenly by allowing the sample to expand under tension, unlike traditional materials. A more compact structure also increases impact strength, making auxetic foams very interesting under high stress. The increased robustness in auxetic foams is due to their ability to maintain stability and prevent structural collapse under stress, which directly enhances their overall toughness compared to traditional foams.

The elastic limit reflects a material's ability to return to its original shape after deformation. Auxetic foams, with their unique structure, can withstand higher stress before reaching their elastic limit, indicating superior performance under mechanical loads. For example, PP-T140-24-P9 exhibits an elastic limit of 120 kPa, a 200% improvement compared to PP-O (40 kPa).

The compressive mechanical properties were also examined, focusing on the modulus and stress at various strains (5% and 50%). The stress–strain curves are presented in Fig. 3 and the corresponding results in Table 3. The modulus of PP-O was higher than most of the auxetic foams, with the exception of PP-T140-24-P9, although the auxetic foams have higher density.

The stress–strain curve for PP-O exhibits three distinct regions: a linear elastic portion, a plateau and exponential

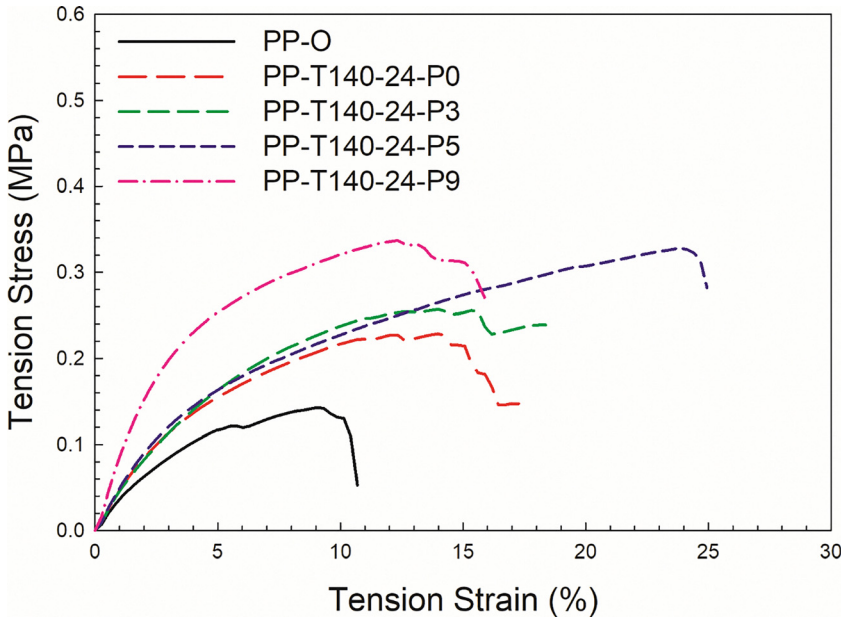

Fig. 2 Tensile stress as a function of tensile strain for the original (PP) and auxetic foams.

Table 2 Tensile properties of the PP auxetic foams produced

Samples	Density (kg m^{-3})	Modulus (kPa)	Strength (kPa)	Strain at break (%)	Toughness (MPa)	Elastic limit (kPa)
PP-O	45	22.2 ± 0.9	149 ± 6	8.6 ± 1.1	1.07	40
PP-T140-24-P0	100	24.6 ± 0.6	228 ± 6	13.9 ± 0.8	2.90	55
PP-T140-24-P3	105	30.8 ± 0.8	257 ± 7	13.3 ± 0.6	3.54	68
PP-T140-24-P5	109	31.4 ± 0.9	324 ± 9	28.7 ± 0.2	5.76	75
PP-T140-24-P9	133	48.3 ± 1.3	337 ± 11	9.8 ± 0.5	4.17	120

growth (Fig. 3). In contrast, the auxetic foams lack a definite plateau region and show only exponential growth. At small deformations ($\leq$5%), the stress and strain are proportional due to cell wall bending. However, the auxetic foams exhibit lower resistance at small deformations because their cell walls are already bent inwards. But above 50% of compression, the foams collapse with negligible stress increase due to buckling of the cell walls. This absence of a plateau region is related to the cell ribs in the re-entrant structure being already bent inwards and bend further rather than buckle. The stress at 50% strain is directly proportional to the amount of material (density) present.

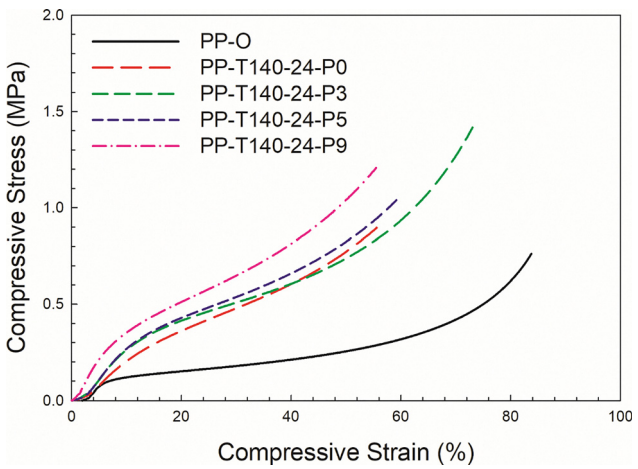

Fig. 3 Compressive stress as a function of compressive strain for the original (PP) and auxetic foams.

Overall, the best performing auxetic foam (PP-T140-24-P9) showed a 416% improvement in stress at 50% strain compared to PP-O. Understanding these mechanical properties and the effect of density provides important insights into the behavior and performance of auxetic foams. This information is important to carefully select their final applications.

For the mechanical properties presented in Fig. 2, 3 and summarized in Tables 2 and 3, it is important to note that the VMC-treated samples may exhibit slight changes in shape and dimensions compared to the untreated PP-O samples. These variations could potentially influence the measured mechanical responses, including tensile strength, strain, and toughness. To account for this effect, the post-treatment dimensions of all samples were carefully measured and reported in Table 1. The measurements were conducted at least 24 h after removal from the oven to ensure full stabilization (thermal and mechanical) of the foam structure. Based on our observations, no noticeable dimensional change occurred after several additional days, confirming that the treated samples reached a stable configuration (equilibrium).

Table 3 Compressive properties of the PP auxetic foams

Samples	Density (kg m^{-3})	Modulus (MPa)	Stress at 5% strain (MPa)	Stress at 50% strain (MPa)
PP-O	45	3.3 ± 0.6	0.07 ± 0.01	0.25 ± 0.09
PP-T140-24-P0	100	1.6 ± 0.4	0.07 ± 0.02	0.77 ± 0.19
PP-T140-24-P3	105	2.2 ± 0.5	0.10 ± 0.03	0.78 ± 0.18
PP-T140-24-P5	109	2.4 ± 0.7	0.12 ± 0.03	0.82 ± 0.24
PP-T140-24-P9	133	4.8 ± 1.1	0.21 ± 0.05	1.04 ± 0.23

This dimensional stability can be attributed to the semi-crystalline nature of PP and its relatively low thermal shrinkage once cooled below its crystallization temperature (the technical specifications data sheet of the producer reports a Thermal stability linear dimensional change $<0.1\%$[27]). The polymer chains in the VMC-treated samples are fixed in the reconfigured cellular geometry during cooling, preventing subsequent relaxation or deformation. Consequently, the dimensional variations after treatment are negligible and do not affect the comparative mechanical testing results. Therefore, improved mechanical performance for the VMC-treated PP foams are mainly associated with structural reconfiguration of the foam cells, rather than differences in sample geometry/dimensions.

3.2.2.2. Thermal–mechanical behavior of auxetic polypropylene foams. The glass transition temperature (T_g) of isotactic polypropylene (PP) is typically observed between −10 °C and 0 °C, while its melting temperature (T_m) lies between 160 °C and 170 °C, depending on the degree of crystallinity and processing conditions.[28] Below T_g, the amorphous regions are rigid and brittle, while above T_g, segmental motion initiates, although the material remains in a solid due to its crystalline phase. The melting process is associated with the disintegration of the crystalline lamellae, with isotactic PP exhibiting a T_m around 165 °C. The onset of crystalline slip and partial amorphization near this temperature corresponds to a pronounced decline in the storage modulus (E').

As temperature increases, the tensile storage modulus (E') of PP progressively decreases, reflecting polymer softening. This reduction arises from enhanced segmental mobility in the amorphous regions and lamellar slip within the crystalline domains, both decreasing the elastic response. At elevated temperatures, partial melting and structural reorganization of the crystalline domains further lower E' (Fig. 4).

Fig. 5 presents the compressive storage modulus (E') of auxetic PP foams as a function of temperature. The E' values of all samples decrease gradually with increasing temperature, reflecting the thermal softening of polypropylene. Compared with the unprocessed PP foam (PP-O), the auxetic foams (PP-140-24-P0 to P9) exhibit significantly higher E' values over the temperature range studied, indicating higher stiffness due to the densified and re-entrant cell structure. E' also increases with the degree of auxetic transformation (from P0 to P9), showing the structural reinforcing effect. A sharp decrease occurs above 120 °C as the material approaches the melting region of the PP crystals.

In auxetic PP foams, cell-wall softening not only affects the polymer matrix, but also decreases the geometric contribution to stiffness, leading to a more rapid decrease in macroscopic E' compared to conventional foams. Nevertheless, auxetic modifications improve the tensile stiffness at low and moderate temperatures, with PP-140-24-P9 exhibiting the highest E' among the tested samples. But at high temperatures (∼100 °C), all the foams display similarly low E' values (∼0.5–1 MPa), indicating that the auxetic structural advantage is lost as the polymer approaches its softening point.

Overall, these results suggest that auxetic foams have better mechanical performance at both ambient and higher temperatures, but this stiffness improvement decreases with increasing temperature.

The results can also be analyzed in terms of $\tan\delta$ (loss tangent), which is the ratio between the loss modulus and storage modulus as measured *via* dynamic mechanical analysis (DMA). This parameter gives information of the damping behavior of materials as required for cushioning, impact strength and vibration dampening. Higher $\tan\delta$ values are associated with higher energy dissipation (more viscous response), while a lower $\tan\delta$ indicates a more elastic behavior. As shown in Fig. 4 and 5, $\tan\delta$ slightly increases with temperature and all samples exhibit a similar trend and values. This behavior is expected because increasing temperature reduces the elastic response and enhances molecular mobility, resulting in higher $\tan\delta$. No distinct inflection point or transition is observed for the samples inside the temperature studied as the range available lies between the glass transition temperature (T_g) and the melting temperature (T_m) of all samples.

In all cases, auxeticity does not seem to modify this parameter as all the curves (treated and untreated samples) have similar values within experimental uncertainty.

3.2.3. Poisson's ratio. A detailed analysis of the PR is presented in the SI. For the sake of brevity, only a general discussion is provided here.

The PR of the PP foams was calculated from tension and compression measurements for both lateral directions: tangential (Y) and thickness (Z), while applying a deformation in the longitudinal direction (X). In this study, the PP foam was rigid and isotropic with a density of 45 kg m^{-3}. The tensile Poisson's ratio was determined to be 0.08 in both directions for tensile elongations up to 10% (Fig. S1). But the average Poisson's ratio in compression was 0.1 in both directions, indicating that the PP foam was isotropic and exhibited higher resistance to deformation in tension compared to compression. This result is different from our previous work on recycled PP foam (density of 28 kg m^{-3}),[7] as a PR of 0.08 was determined in compression with a value of 0.28 in tension. However, Rinde reported that for strains below 10%, the tensile Poisson's ratio of PP foams was 0.25, with higher values in tension than in compression, the latter being close to zero.[29] These differences must be related to the foam morphology.

For the auxetic foams shown in Fig. S2, the PR was negative below 25% of tensile strain. The Poisson's ratio increased with increasing engineering strain, although the curves do not show a linear dependence with axial strain. This behavior is consistent with the results of Evans *et al.*[30] and Lake *et al.*,[9] although

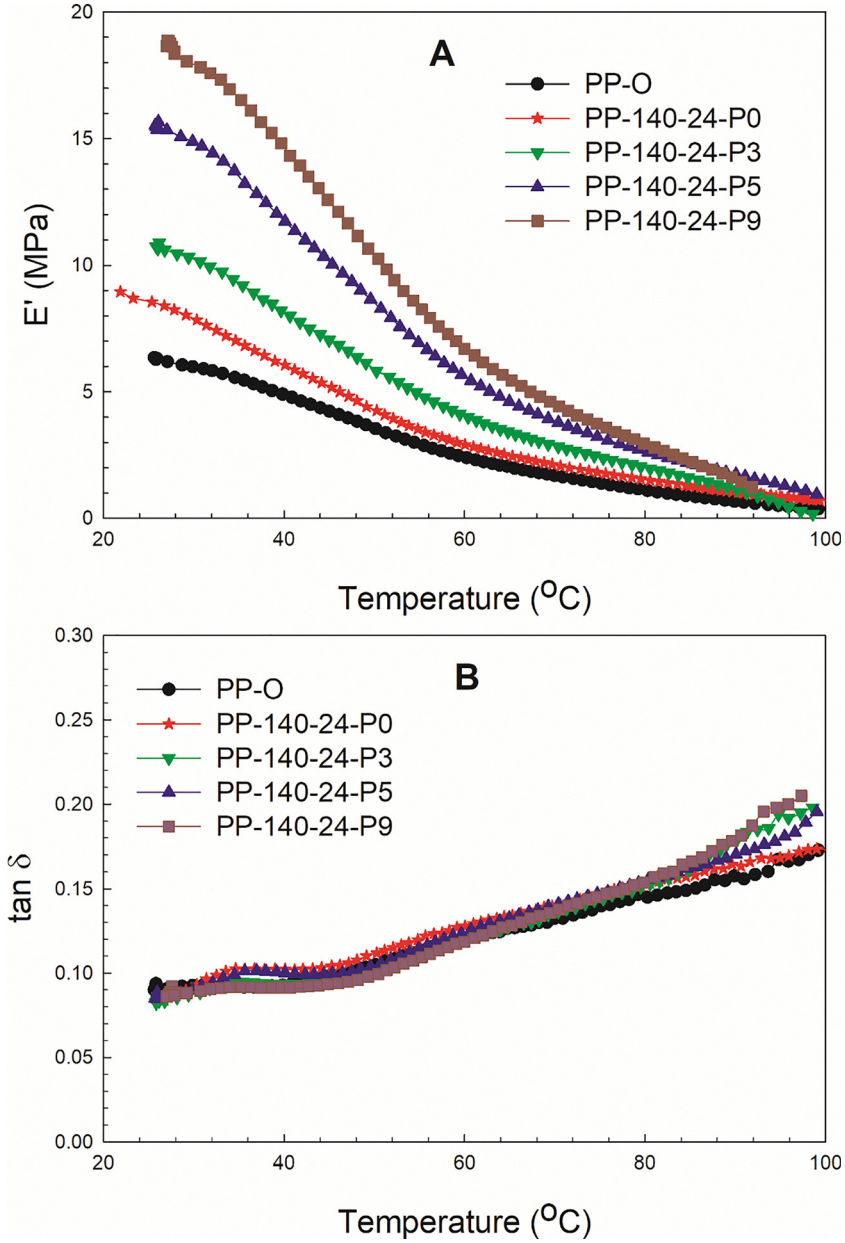

Fig. 4 (A) Tensile storage modulus (E') and (B) tan δ of auxetic PP foam as a function of temperature.

different materials were used (expanded polytetrafluoroethylene and mixed polyurethane–polyester foam, respectively) with very different structures. This trend was reported for NPR foams.[8,30–32]

Fig. 6 presents a series of images at different time (2 s to 150 s) for three polypropylene (PP) samples (PP-O, PP-140-24-P5 and PP-140-24-P3) under tensile loading (1.2 mm min^{-1}). The deformation of each sample is presented, including changes in both width and length as a function of time. For each image, Table 4 reports the length, width and corresponding instantaneous Poisson's ratios (PR or NPR) as determine by ImageJ. PP-O (conventional PP) increases its length from 30.0 mm to 33.0 mm over the time period (2–150 s), while its width decreases from 12.9 mm to 12.7 mm leading to positive Poisson's ratio (from 0.07 to 0.18), which is consistent with conventional materials. On the other hand, PP-140-24-P3 and PP-140-24-P5 (treated samples) show increases in both length and width over time. For example, the length of PP-140-24-P3 increases from 25.0 to 28.3 mm, while the width increases from 12.17 to 12.41 mm. This behavior corresponds to a negative Poisson's ratio (NPR) reaching values as low as −0.33. For PP-140-24-P5, the values are slightly less negative (down to −0.23). This indicates that the material is auxetic, but to a lower extent compared to PP-140-24-P3. These results show that the VMC method was successful to produce NPR foams, and that the treatment conditions control the final auxetic properties from the foams' morphology being different than the original sample.

Fig. 7 illustrates the tensile deformation behavior of the original PP foam (PP-O) and a typical auxetic foam (PP-140-24-P3) at

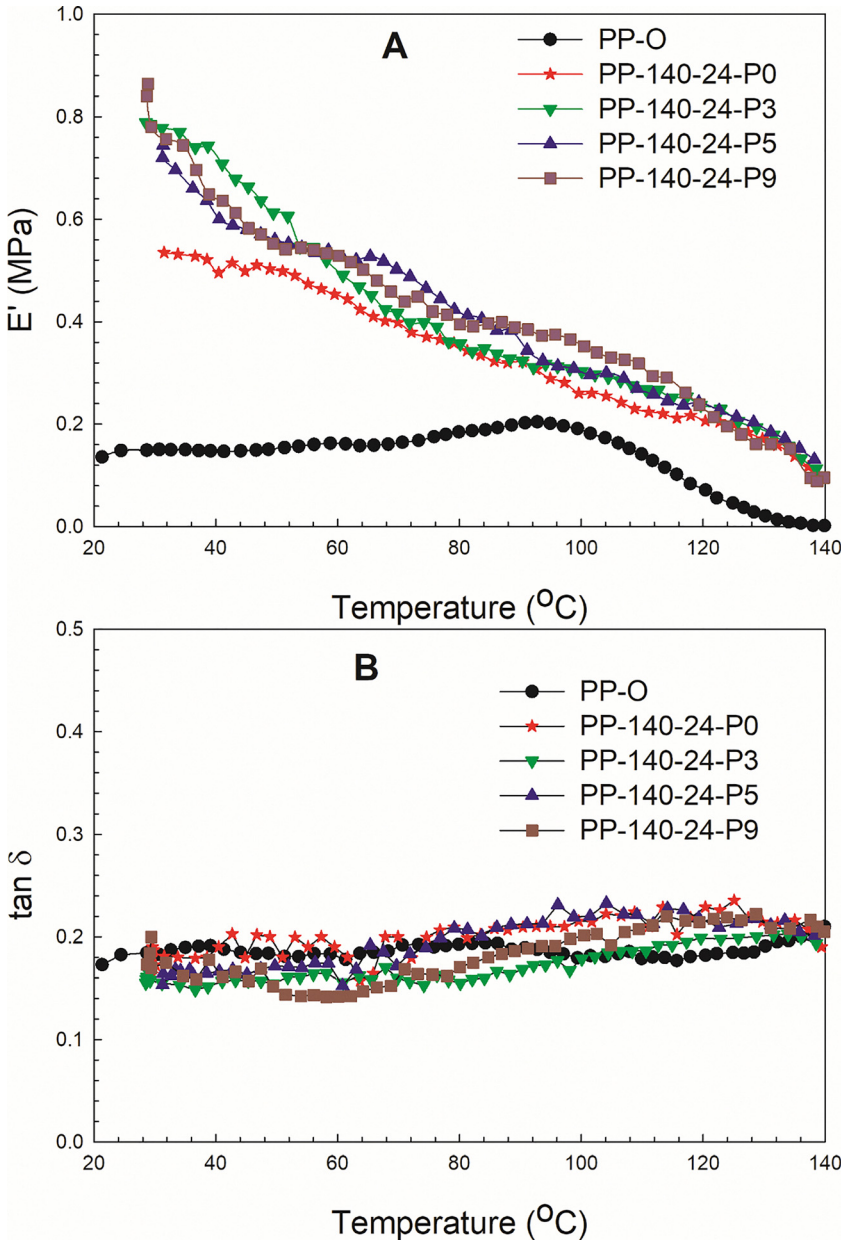

Fig. 5 (A) Compressive storage modulus (E') and (B) tan δ of auxetic PP foam as a function of temperature.

selected time intervals. For each sample, the evolution of length and width is shown during uniaxial tensile loading. The original PP foam exhibits a slight lateral contraction as the length increases, corresponding to a small, but positive, Poisson's ratio. On the other hand, the auxetic foam shows a slight lateral expansion during tensile deformation, indicating a negative Poisson's ratio.

Because the absolute values of Poisson's ratio are small, the visual differences between samples are small. However, the measured dimensional changes are consistent with the Poisson's ratio values reported in Table 6, a conformation of the transition from conventional to auxetic behavior after thermo–mechanical treatment. Nevertheless, the figure is presented only to qualitatively illustrate this behavior, while quantitative confirmation is provided by the measured Poisson's ratios. To better visualize the material modifications, Fig. 7 compares PP-O and PP-140-24-P3 in terms of the time evolution of sample dimensions (length and width) under tensile deformation. Because each sample has its own characteristic scale, the length and width at each time point are reported directly in the figure.

For the original PP foam, the PR was positive (0.08). For the treated samples, the results are very similar: PP-T140-24-P5 and PP-T14-24-P9 are almost identical with a minimum NPR of −0.08 (in Table 5, the values reported are the average of a minimum of three samples). The PR increased with compressive engineering strain and remained negative up to a strain of 15–20%, before increasing to zero and 0.05. This trend is consistent with the findings of Choi *et al.*[31] and Lisieck

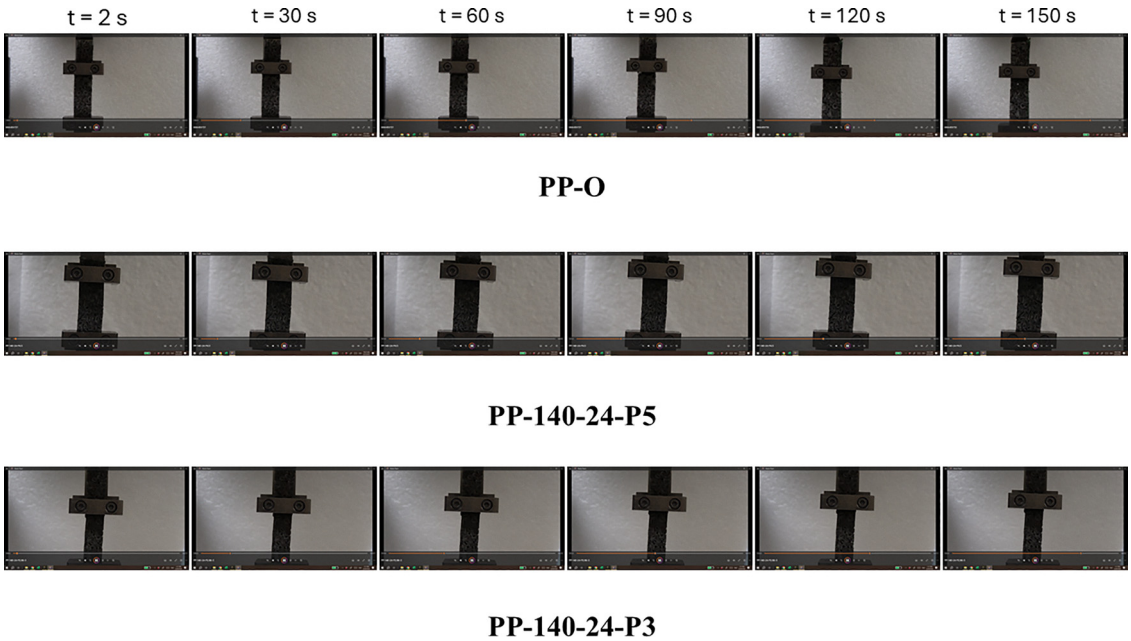

Fig. 6 Typical images of selected samples (PP-O, PP-140-24-P5 and PP-140-24-P3) as a function of time under tensile deformation (1.2 mm min^{-1}).

Table 4 Length and width of selected samples at various time, along with their corresponding Poisson's ratios

	PP-O			PP-140-24-P3			PP-140-24-P5		
Time (s)	Length (mm)	Width (mm)	PR (–)	Length (mm)	Width (mm)	NPR (–)	Length (mm)	Width (mm)	NPR (–)
2	30.0	12.9	—	25.0	9.41	—	25.0	12.17	—
30	30.6	12.9	0.07	25.5	9.46	−0.23	25.5	12.27	−0.33
60	31.2	12.8	0.18	26.4	9.51	−0.22	26.4	12.30	−0.17
90	31.8	12.8	0.15	27.1	9.56	−0.23	27.1	12.33	−0.17
120	32.4	12.7	0.17	27.3	9.55	−0.16	27.3	12.34	−0.14
150	33.0	12.7	0.14	28.3	9.53	−0.11	28.3	12.41	−0.16

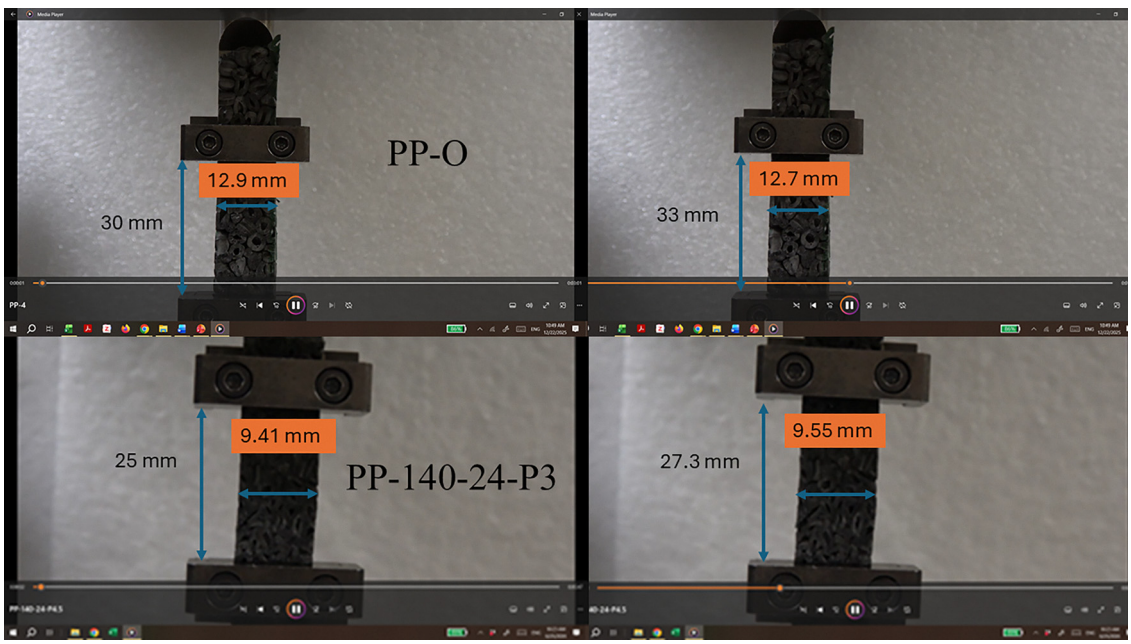

Fig. 7 Comparison between PP-O and PP-140-24-P3 in terms of dimensions changing with time under tensile deformation (constant rate of 1.2 mm min^{-1}).

Table 5 Properties of the auxetic samples based on PP foams

Sample	Final density (kg m^{-3})	Compression ratio (ρ_f/ρ_o)	Minimum PR (tension)	Minimum PR (compression)
PP-O	45	1	0.08 (average)	0.1 (average)
PP-T140-24-P0	100	2.2	−0.12	−0.03
PP-T140-24-P3.0	103	2.3	−0.23	−0.06
PP-T140-24-P5.0	126	2.8	−0.22	−0.08
PP-T140-24-P9.0	132	2.9	−0.18	−0.08

Table 6 Comparison of the properties of PP auxetic foams with results from the literature

Raw foam density (kg m^{-3})	Treated density (kg m^{-3})	Minimum PR (tension)	Minimum PR (compression)	Ref.
PP foam-28	116	−1.50	−0.28	7
PP/NaCl*	—	−0.46	—	33
PP foam-45	103	−0.23	−0.06	This work

et al.,[32] despite their original materials being a mixture of closed and open-cell polyurethane-polyester foam (density of 30 kg m^{-3}) and open-cell PU foam (density of 25 kg m^{-3}). The relationship between axial compressive strain and PR is non-linear due to the complex interplay between the re-entrant structure (cell geometry and size), imposed deformation and resulting Poisson's ratio.

To the best of our knowledge, there is no study on auxetic materials produced from polypropylene foams using post-processing approaches similar to this work, except for our earlier study.[7] It was reported that Poisson's ratios under tensile loading (−0.8 to −1.5) and compressive loading (−0.02 to −0.32) were achieved. These values were obtained using lower density waste PP foams (28 kg m^{-3}), which were easier to deform and therefore more prone to pronounced auxetic behavior.

For comparison, Table 6 now includes results from the literature, especially the study ''preparing polypropylene auxetic foam by a one-pot CO_2 foaming process'', where auxetic behavior was achieved by direct foaming. In this case, the Poisson's ratio ranged from −0.13 to −0.46. Since the auxetic structures were generated through fundamentally different processing methods (direct foaming *vs.* post-processing), a direct quantitative comparison is not straightforward.

4. Conclusion

This study successfully transformed conventional polypropylene (PP) foams into auxetic metamaterials using a vacuum and mechanical compression (VMC) method. The process involved heat treatment, vacuum application and mechanical pressure, resulting in a re-entrant cellular structure crucial to generate a negative Poisson ratio (NPR). The optimized auxetic foams exhibited increased density, reduced porosity and a significantly enhanced toughness compared to the original PP foams. For example, sample PP-T140-24-P5 had a toughness of 5.76 MPa, which is 438% higher than the original foam, with a 200% improvement of the elastic limit. On the other hand, the stress at 50% compressive strain of PP-T140-24-P9 (1.04 MPa) was improved by 416% compared to the original foam (0.25 MPa).

The tensile and compressive storage moduli (E') of PP-T140-24-P9 have a substantial improvement of 189% (18.4 MPa) and 433% (0.86 MPa) at ambient temperature compared to the original foam (6.3 MPa, 0.14 MPa), respectively.

The PR of the treated samples was found to stay negative up to 25% strain in tension (minimum of −0.23) and up to 20% of strain in compression (minimum of −0.08). These results confirm the efficiency of the re-entrant cellular morphology obtained. The auxetic foams also displayed improved tensile strength (from 228 kPa to 337 kPa) and elongation at break (from 8.6% to 28.7%), indicating better ductility.

These enhanced properties make auxetic PP foams highly suitable for applications requiring robust and high-performance materials, such as sports and military protection equipment. Auxetic foams can also be applied in a wide range of applications such as medical prosthetics and orthotics, aerospace, construction and sports equipment, due to their flexibility, durability and resistance.

Finally, future work should further explore the treatment conditions to optimize these parameters and investigate the potential applications of these auxetic foams across various fields. More characterization should also be performed including fatigue, creep, relaxation and impact resistance.

Conflicts of interest

The authors declare no conflict of interest.

Data availability

All data generated or analyzed during this study are included in this published article and its supplementary information (SI) files. Supplementary information is available. See DOI: https://doi.org/10.1039/d5ma01329a.

References

1 R. S. Lakes, *Annu. Rev. Mater. Res.*, 2017, **47**, 63–81.
2 W. Jiang, X. Ren, S. L. Wang, X. G. Zhang, X. Y. Zhang, C. Luo, Y. M. Xie, F. Scarpa, A. Alderson and K. E. Evans, *Composites, Part B*, 2022, **235**, 109733.
3 M. F. Fardan, B. W. Lenggana, U. Ubaidillah, S.-B. Choi, D. D. Susilo and S. Z. Khan, *Micromachines*, 2023, **14**, 1165.
4 M. F. Ahmed, Y. Li and C. Zeng, *Mater. Chem. Phys.*, 2019, **229**, 167–173.
5 N. Chan and K. E. Evans, *J. Mater. Sci.*, 1997, **32**, 5945–5953.
6 X. Y. Chen and D. Rodrigue, *Macromol. Rapid Commun.*, 2025, **46**, e2400274.
7 X.-Y. Chen and D. Rodrigue, *Macromol*, 2023, **3**, 463–476.

8 X. Y. Chen and D. Rodrigue, Conversion of polystyrene foams into auxetic metamaterials, *Polym. Eng. Sci.*, 2023, **63**, 2193–2203.
9 R. Lakes, *Science*, 1987, **235**, 1038–1040.
10 M. Bianchi, F. L. Scarpa and C. W. Smith, *J. Mater. Sci.*, 2008, **43**, 5851.
11 M. Bianchi, F. Scarpa, M. Banse and C. W. Smith, *Acta Mater.*, 2011, **59**, 686–691.
12 M. Bianchi, F. Scarpa and C. W. Smith, *Acta Mater.*, 2010, **58**, 858–865.
13 M. Bianchi, S. Frontoni, F. Scarpa and C. W. Smith, Density change during the manufacturing process of PU–PE open cell auxetic foams, *Phys. Status Solidi B*, 2011, **248**, 30–38.
14 Q. Zhang, W. Lu, F. Scarpa, D. Barton, R. S. Lakes, Y. Zhu, Z. Lang and H.-X. Peng, *Appl. Mater. Today*, 2020, **20**, 100775.
15 Q. Zhang, W. Lu, F. Scarpa, D. Barton, K. Rankin, Y. Zhu, Z.-Q. Lang and H.-X. Peng, *Mater. Des.*, 2021, **211**, 110139.
16 Q. Zhang, X. Yu, F. Scarpa, D. Barton, K. Rankin, Z.-Q. Lang and D. Zhang, *Composites, Part B*, 2022, **237**, 109849.
17 D. Fan, M. Li, J. Qiu, H. Xing, Z. Jiang and T. Tang, *ACS Appl. Mater. Interfaces*, 2018, **10**, 22669–22677.
18 O. Duncan, T. Allen, A. Birch, L. Foster, J. Hart and A. Alderson, *Smart Mater. Struct.*, 2021, **30**, 015031.
19 O. Duncan, G. Leslie, S. Moyle, D. Sawtell and T. Allen, *Smart Mater. Struct.*, 2022, **31**, 074002.
20 E. O. Martz, T. Lee, R. S. Lakes, V. K. Goel and J. B. Park, *Cell. Polym.*, 1996, **15**, 229–249.
21 X. Y. Chen, R. S. Underhill and D. Rodrigue, *Appl. Sci.*, 2023, **13**, 1148.
22 McMaster-Carr, https://www.mcmaster.com/, (accessed November 7, 2025).
23 R. Critchley, I. Corni, J. A. Wharton, F. C. Walsh, R. J. K. Wood and K. R. Stokes, *Phys. Status Solidi B*, 2013, **250**, 1963–1982.
24 L. Andena, F. Caimmi, L. Leonardi, M. Nacucchi and F. De Pascalis, *J. Cell. Plast.*, 2019, **55**, 49–72.
25 D. Li, L. Zhou, X. Wang, L. He and X. Yang, *Materials*, 2019, **12**, 1746.
26 A. Bezazi and F. Scarpa, *Int. J. Fatigue*, 2009, **31**, 488–494.
27 McMaster Part Number 9107T11= IAFPOLYP1024G, Technical Specifications data sheet.
28 J. E. Mark, *Polymer Data Handbook*, Oxford University Press, Oxford, New York, 2nd edn, 2009.
29 *J. Appl. Polym. Sci.*|Wiley Online Library, DOI: 10.1002/app.1970.070140801, (accessed November 7, 2025).
30 B. D. Caddock and K. E. Evans, *J. Phys. D: Appl. Phys.*, 1989, **22**, 1877.
31 J. B. Choi and R. S. Lakes, *J. Mater. Sci.*, 1992, **27**, 4678–4684.
32 J. Lisiecki, T. Błażejewicz, S. Kłysz, G. Gmurczyk, P. Reymer and G. Mikułowski, *Phys. Status Solidi B*, 2013, **250**, 1988–1995.
33 N. Li, Z. Liu, X. Shi, D. Fan, H. Xing, J. Qiu, M. Li and T. Tang, *Adv. Eng. Mater.*, 2022, **24**, 2100859.